British Journal of Pharmacology (2000) 131, 1275–1284

www.nature.com/bjp

Block of the lymphocyte K^+ channel *m*Kv1.3 by the phenylalkylamine verapamil: Kinetic aspects of block and disruption of accumulation of block by a single point mutation

[1]Raphael J. Röbe & *,[1]Stephan Grissmer

[1]Department of Applied Physiology, University of Ulm, Albert-Einstein-Allee 11, 89081 Ulm, Germany

1 Phenylalkylamines (PAA) usually known for their action on L-type Ca^{2+} channels potently block the C-type inactivating lymphocyte Kv1.3 channel resulting in inhibition of activation of T lymphocytes. In order to design PAAs blocking Kv1.3 specifically over L-type Ca^{2+} channels, we investigated the state-dependent manner of *m*Kv1.3 block by the PAA verapamil.

2 Verapamil seems to have access to the open state (OB) and, once bound to the channel, the channel-verapamil complex is absorbed into a slowly recovering state. This state was proposed to be the inactivated blocked state (IB). Here we present a quantitative description of the transition into this state and provide evidence for the IB state through experiments with an inactivation lacking mutant channel. Since the inactivated state cannot be reached in this case the IB state cannot be reached either.

3 We show that the transition OB→IB is accelerated by verapamil most likely through a mechanism involving the reduction of $[K^+]$ at an inactivation modulating low affinity binding site for K^+ at the outer vestibule.

4 Measurements of the voltage-dependence of the off-rate constants for verapamil suggest that verapamil can reach the channel in its neutral form and might get partially protonated while bound. Thus only those verapamil molecules that are protonated can more easily dissociate at hyperpolarizing voltages.

5 Since open block kinetics were shown to be similar for wild type *m*Kv1.3 and the H404T mutant *m*Kv1.3 channel, and since the block of the H404T mutant channels by verapamil could be described exactly by a simple three-state open block model, the mutant channel could serve as a screening channel to determine open block affinities of new PAA derivatives in high through-put experiments. *British Journal of Pharmacology* (2000) **131,** 1275–1284

Keywords: Lymphocyte K^+ channel; *m*Kv1.3; phenylalkylamine; verapamil; accumulation of block; inactivation; kinetic model

Abbreviations: acc, accumulated; C, closed state, DEPC, diethylpyrocarbonate; DMSO, dimethylsulphoxid; I, inactivated state; IB, inactivated, blocked state; O, open state; OB, open, blocked state; PAA, phenylalkylamines; RBL, rat basophilic leukemia; TEA, tetraethylammonium

Introduction

The *m*Kv1.3 channel is a member of the family of voltage-gated, delayed rectifier K^+ channels and of the subfamily of the *Shaker*-related channels. It is composed of six membrane spanning segments and a so called P-loop between segment 5 and 6 (Durell & Guy, 1996). The major physiological role of Kv1.3 channels (homologous to *n*-type channels of lymphocytes; Grissmer *et al*., 1990) known so far is to generate and maintain a negative membrane potential in T lymphocytes during activation (Chandy *et al*., 1984; 1993). Block of *m*Kv1.3 has been shown to result in a diminished Ca^{2+} influx into the T cell, resulting in a lack of lymphokine production and an attenuated immune response, as shown in mini-pig (Koo *et al*., 1997).

In humans, the use of *m*Kv1.3-blocking substances could also be clinically useful, for example in treatment of transplant reactions or autoimmune disorders (Cahalan & Chandy, 1997). One candidate group for the block of Kv1.3 are the phenylalkylamines (PAA), which are known as one entity of the classical L-type Ca^{2+} channel blockers (beside the benzothiazepines and the dihydropyridines) and clinically used as antiarrhythmic and antihypertensive drugs over decades without severe side-effects. Therefore the binding properties at the K^+ channel need to be investigated in order to produce new PAA-derivatives, which are Kv1.3-selective over L-type Ca^{2+} channels.

The intrinsic channel properties of *m*Kv1.3 are well known (investigated by DeCoursey *et al*., 1984, Cahalan *et al*., 1985 and DeCoursey, 1990) showing voltage-dependent activation upon depolarization within a few milliseconds and voltage-dependent (~-38 mV per e-fold) deactivation. Deactivation is slower the higher $[K^+]_o$. C-type inactivation is present with time constants varying from 200 to 800 ms depending on $[K^+]_o$ (DeCoursey, 1990). Block of *m*Kv1.3 by the PAA verapamil was described by DeCoursey (1995) and Jacobs & DeCoursey (1990) as a state-dependent open channel block with the possibility of accumulation resulting from the transition of blocked channels into an absorbing state (a non-conducting state from which recovery was slow). DeCoursey (1995) proposed that this absorbing state was the inactivated blocked state. Here we show additional evidence that it is in fact the postulated state and that this inactivated state is accessible and has affinity to verapamil similar to the open state.

*Author for correspondence;
E-mail: stephan.grissmer@medizin.uni-ulm.de

In comparison, for the block of L-type Ca^{2+} channels by PAA some more mechanistic approaches had restricted the PAA binding site to the fourth domain of the α_1-subunit *via* photoaffinity-labelling (Striessnig *et al*., 1990). The D888 binding site, the so-called high affinity binding site, could be localized to IV S6 (Y1463, A1467, I1470), III S6 (Y1152) and to two negatively charged amino acids in the P-loops of segments III and IV (E1118, E1419) *via* single amino acid mutation (Hockerman *et al*., 1995; 1997). Another approach, to gain kinetic insight, was to simulate PAA-block with wild type and mutant L-type Ca^{2+} channels by different models. Johnson *et al*. (1996) proposed a model with weak block of closed channels and similar affinities for activated and inactivated states. Also Hering *et al*. (1997) pointed out the importance of the inactivation for PAA-block of L-type channels reaching a 'deep' inactivated channel conformation responsible for accumulation of block.

In *m*Kv1.3 channels, however, the role of inactivation in the accumulation of verapamil block was unclear (compare DeCoursey, 1995 vs Rauer & Grissmer, 1999). Here we show results and propose a kinetic model, where inactivation is essential in accumulation of verapamil-block and we describe a mutant *m*Kv1.3 channel, which does not inactivate and also can not accumulate block. Therefore, we could explain the different blocking behaviors of wild type and mutant channels with differences in their intrinsic inactivation properties. This mutant channel could now be used to simplify measurements of block rates by PAAs on *m*Kv1.3 and would therefore make screening experiments with new PAA derivatives possible. In addition, experiments with double mutants (H404T + XnnnY) could now be envisioned trying to identify the verapamil binding site at the channel.

Some of the results have been reported in preliminary communications (Röbe & Grissmer, 1999; 2000).

Methods

Cells

The experiments were performed with single cells (cell line: rat basophilic leucemia, RBL; Eccleston *et al*., 1973). Cells were obtained from the American Type Culture Collection (Rockville, M.D., U.S.A.). The cells were maintained in a culture medium of MEM supplemented with 1 mM L-glutamin and 10% heat-inactivated foetal calf serum in a humidified, 5% CO_2, incubator at 37°C. Cells were plated to grow non-confluently onto glass one or two days prior to use for injection and electrophysiological experiments.

Solutions

Cells were bathed during the experiments in either mammalian Na^+-Ringer's solution (in text: high $[Na^+]_o$), containing in mM: NaCl 160; KCl 4.5; $CaCl_2$ 2; $MgCl_2$ 1; HEPES 5; NaOH ad pH 7.4 with an osmolarity of 290–320 mOsm, or in K^+-Ringer's solution (in text: high $[K^+]_o$), containing in mM: KCl 164.5; $CaCl_2$ 2; $MgCl_2$ 1; HEPES 5; KOH ad pH 7.4 with the same osmolarity. The temperature of the solutions during the experiments was 21–25°C. A simple syringe-driven perfusion system was used to exchange the bath solutions in the recording chamber. For one experiment a fast change in the local verapamil-concentration was necessary, therefore a pico-spritzer system was used (Pico-spritzer II, General valve, New Jersey, U.S.A.). This system was evaluated by blowing a high $[K^+]_o$ containing pipette solution onto the cell while the cells was bathed in high $[Na^+]_o$ (holding potential −20 mV). The amount of change in local $[K^+]_o$ could be estimated by the shift in reversal potential. As the direction of K^+ current went from outward to inward, we were sure that the reversal potential was more positive than −20 mV, indicating a rather complete exchange of local bath, which was obtained within 80 ms.

The internal pipette solution for whole cell recording was in mM: KF 155, $MgCl_2$ 2, HEPES 10, EGTA 10, KOH ad pH 7.2 with an osmolarity of 290–320 mOsm.

Chemicals

The phenylalkylamine verapamil was purchased from Sigma-Aldrich Chemie (Deisenhofen, Germany) as the racemate ± verapamil hydrochloride, dissolved in DMSO (dimethylsulphoxid; FLUKA Chemie AG, Buchs, Germany) as a stock solution, from which the final solutions were diluted in order to keep the final bath solution at a DMSO concentration of <0.1%. The stock solution was kept light protected at 4°C.

Electrophysiology

All experiments were performed in the whole-cell mode of the patch clamp technique as described earlier (Hamill *et al*., 1981; Rauer & Grissmer, 1996; 1999). The electrodes were glass capillaries purchased from Clark Elektromedical Instruments (Reading, U.K.) which were pulled in two stages by a DMZ-Puller (Zeitz, Augsburg, Germany), coated with Sylgard (Dow Corning, Seneffe, Belgium) and fire-polished to final resistances of 3–5 MΩ. The membrane currents were recorded with an EPC-9 patch-clamp amplifier (HEKA elektronik, Lambrecht, Germany) interfaced to a Macintosh computer Quadra 840AV with the acquisition and analysis software Pulse and PulseFit (HEKA elektronik, Lambrecht, Germany). Capacitative and leak currents were subtracted (except if indicated otherwise in the text) using the P/8 procedure. A series resistance compensation (80–90%) was employed if the current amplitude exceeded 1 nA. Holding potential was usually -80 mV (if not mentioned otherwise), depolarizing potential was to 40 mV.

Expression

The *m*Kv1.3 wild type gene and the *m*Kv1.3 H404T mutant gene (a generous gift from Dr K. George Chandy, University of California, Irvine, U.S.A.), embedded in the vector pSP 64T (Krieg & Melton, 1984), were linearized with *Eco*RI (MBI Fermantas, St. Leon-Rot, Germany) and *in-vitro* transcribed with the SP6 Cap-Scribe system (Boehringer Mannheim, Germany). The cRNA could be stored up to 6–8 months at −75°C in H_2O-DEPC (diethylpyrocarbonate) after purification with phenol/chloroform.

Injection

After diluting the cRNA (1–5 $\mu g\ \mu l^{-1}$) with a fluorescent FITC (0.5–2% FITC-Dextran in 100 mM KCl) to a concentration of 0.2–2.5 $\mu g\ \mu l^{-1}$, the solution was injected into the RBL cells using a microinjection system (Micromanipulator 5171 and Transjector 5246 by Eppendorf, Hamburg, Germany) and the injection capillaries (Femtotips, Eppendorf, Hamburg, Germany). After a 3–6 h incubation, the injected cells could be identified by the FITC under fluorescent light and specific currents could be elicited.

Fits and simulation

This section refers particularly to the data presented in Figure 6 and Table 1. Inactivation time constants, current decay time constants, steady-state currents and time constants for the tail integrals were fitted by using the computer fitting routine of PulseFit and Igor (Vers. 1.27, Wave-Metrics, Lake Oswego, U.S.A.). Time constants for recovery from inactivation and recovery from block were deduced from fitting mono- or bi-exponential functions by eye. For the recovery curves the fractional recovery (fr) was used as $fr = (I_{peak\ 2} - I_{ss\ 2})/(I_{peak\ 1} - I_{ss\ 1})$, where I is the current, either peak or steady-state (ss) of each pulse (Levy & Deutsch, 1995). The fit was done according to the mono-exponential function: $fr = 1-(\exp(-IPI/\tau_{rec}))$ and the bi-exponential function: $fr = 1-(A_f*\exp(-IPI/\tau_{rec\ f}) + A_s*\exp(-IPI/\tau_{rec\ s}))$, where IPI is the interpulse interval, $\tau_{rec\ s}$ and $\tau_{rec\ f}$ are the time constants of the function, A_f and A_s are the fractions of the fast and slow recovering channels, respectively ($A_f + A_s = 1$).

To recreate the current decay of inactivation and block and to check the predictions of the model, we simulated the channel states according to scheme I (wild type) or II (H404T mutant) shown in Figure 1, so that state O overlays the original normalized current. The transitions between the states are defined by the following differential equations:

$$d\,C/dt = 4\beta * O - \alpha * C$$
$$d\,O/dt = \alpha * C - 4\beta * O - k' * O - h * O + l * OB + j * I$$
$$d\,I/dt = h * O - j * I - k' * I + l * IB$$
$$d\,OB/dt = k' * O - l * OB - h^* * OB + j^* * IB$$
$$d\,IB/dt = h^* * OB + k' * I - j^* * IB - l * IB$$

The respective rate constants were deduced from fitting the original currents or adjusted manually during the simulation, according to the following methods: (i) α was obtained during depolarization by fitting the onset of current without verapamil, regarding only the fourth constant of the Hodgkin–Huxley model ($\alpha = 1\alpha$); during repolarization α was set to 0. (ii) 4β was deduced from $1/\tau_{tail}$ for each repolarizing voltage used, regarding only the first constant of the Hodgkin-Huxley model ($4\beta = \beta$); during depolarization β was set to 0. (iii) k' was deduced from $1/\tau_{corr}$, where τ_{corr} is the time constant of the current decay in the presence of verapamil, τ_{decay}, corrected for the endogenous inactivation in wild type: $\tau_{corr} = 1/(1/\tau_{decay} - 1/\tau_{inact})$. From k' we also deduced k as $k = k'\ [Ver]^{-1}$. If a significant steady-state current during depolarizations was detectable, k was corrected for the off-rate constant l, according to $l = 1/(R^*\tau_{corr})$, where R is the ratio of the steady-state current in the presence of verapamil and the peak current in the absence of verapamil. For the simulations during repolarization we assumed a voltage dependence of k of 138 mV per e-fold (DeCoursey, 1995). (iv) $l_{(-80\ to\ -160\ mV)}$ was deduced from the corresponding tail currents ($l = 1/\tau_{tail}$); because unblock is slower than deactivation, the time constant of a mono-exponential fit to the tail current reflects mainly the residency time of verapamil. If unblock resulted in hooked currents, the second, declining part was used for the fit. (v) $l_{(40\ mV)}$ was manually adjusted during simulation (wild type) or deduced from the steady-state currents during depolarization (H404T mutant), according to: $l = 1/(R^*\tau_{corr})$. (vi) K_d is the ratio l/k at 40 mV. (vii) h was deduced from fitting a mono-exponential function (τ_{inact}) to the currents decay in wild type in the absence of verapamil and was assumed to be voltage independent (DeCoursey, 1990). In the H404T mutant channels h was set to 0 in the simulations. (viii) j was obtained from $1/(R^*\tau_{inact})$, where R is the ratio of the steady-state current and the peak current and τ_{inact} is the inactivation time constant. During repolarization we deduced j from $1/\tau_{rec}$, where τ_{rec} is the time constant of the mono-exponential recovery fit. Thus, inactivation is assumed to have a mono-exponential time course with a non-inactivating fraction R. (ix) h^* was deduced in high $[K^+]_o$ from the mono-exponential fit ($\tau_{inact\ vera}$) of the decay of the tail currents' integrals in the presence of verapamil (Figure 4): $h^* = 1/\tau_{inact\ vera}$. In high $[Na^+]_o$ h^* was adjusted manually during the simulation. In the H404T mutant channels h^* was set to 0 for the simulations. (x) j^* resulted from the conservation of energy in the model circuit: $j^* = (k * h^* * l * j)/(l * h * k')$ in high $[K^+]_o$; in high $[Na^+]_o$ j^* was adjusted deviating from the maintenance of the microscopic reversibility, because we could not be sure that the recovery path is *via* the O-state only (Marom & Levitan, 1994).

Thus, in the simulation in high $[K^+]_o$ the only variable during repolarization was l, during repolarization no variable existed, so that the model predicts the recovery from block, given by the state C. In high $[Na^+]_o$, h^*, l and j^* had to be adjusted because tail currents after steady-state block could not be seen.

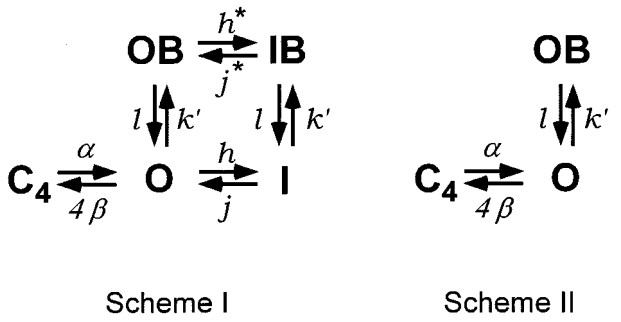

Figure 1 Simplified scheme of Kv1.3 transitions by depolarization in the absence and presence of verapamil with (scheme I, for wild type *m*Kv1.3 channels) and without (scheme II, for H404T mutant *m*Kv1.3 channels) C-type inactivation.

Results

Block of wild type *m*Kv1.3 by verapamil is characterized by two distinguishable phenomena: (i) An acceleration of current decay during depolarizations probably representing state-dependent block of open channels and (ii) an accumulation of block at pulse frequencies where accumulation did not result from the slow recovery from intrinsic inactivation (DeCoursey, 1995; Rauer & Grissmer, 1996). Figure 2 shows these two characteristic features of verapamil block under different conditions. In Figure 2A, a control current through *m*Kv1.3 in the absence of verapamil in a high $[Na^+]_o$ containing solution is shown with its typical C-type inactivation ($\tau_{inact} = 220 \pm 91$ ms; $n = 42$). When verapamil was added to the bath solution, current decay was accelerated without an effect on the activation time course. Peak current was smaller in the presence of verapamil and the following pulses elicited currents with similar accelerated decays but further reductions of peak currents, which decreased from pulse to pulse until the peak current was reduced to about a third of the control peak current. The time course of the peak current reduction following each pulse can be seen in Figure 2B. Using high $[K^+]_o$ as the bathing solution differences in the verapamil block characteristics can be observed compared to

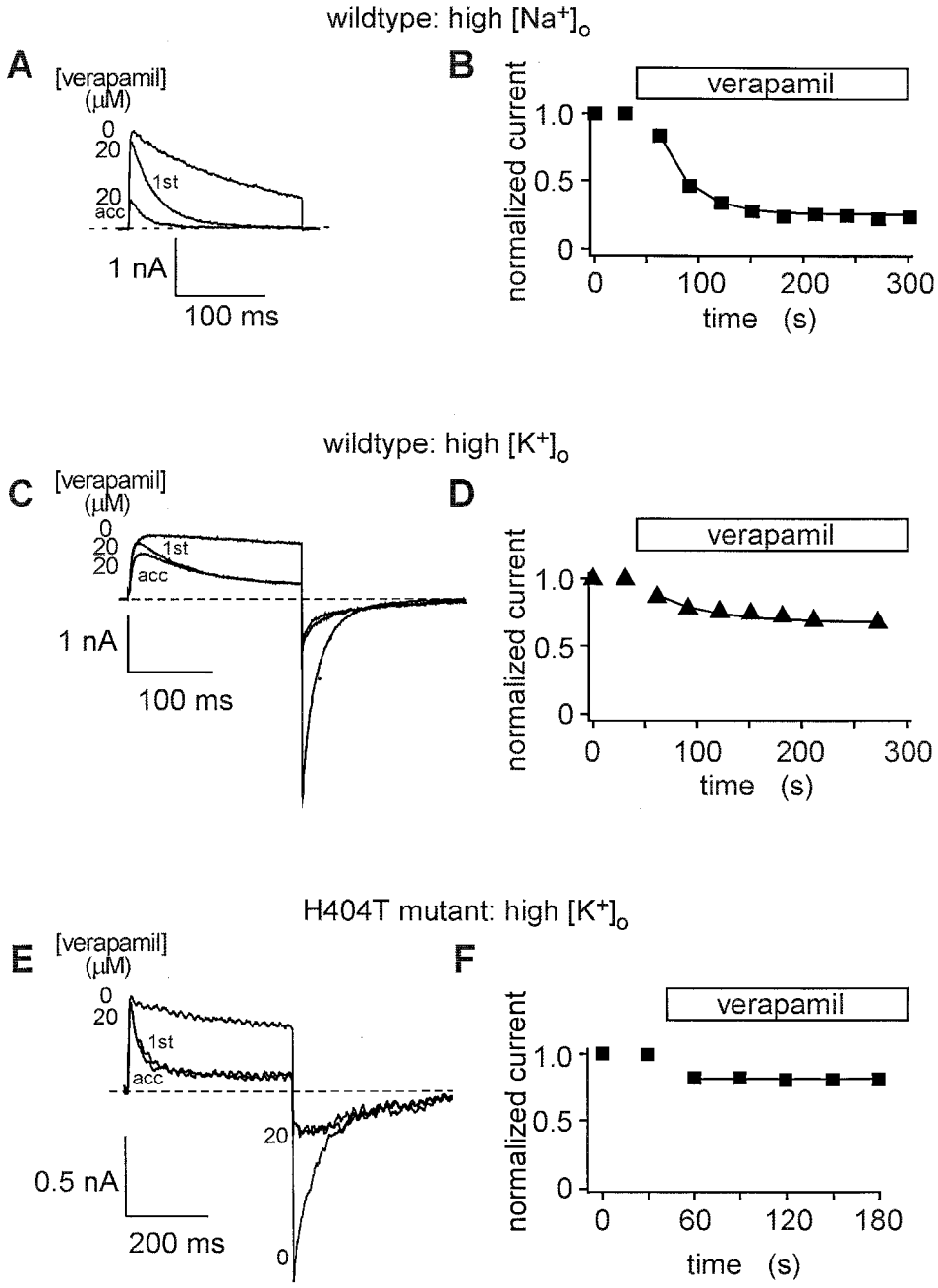

Figure 2 Basic properties of verapamil to block current through wild type and mutant H404T *m*Kv1.3. Currents were elicited with depolarizations to 40 mV from a holding potential of −80 mV in the absence (control) and presence of 20 μM verapamil in the bath solution which was either high $[Na^+]_o$ (A, B) or high $[K^+]_o$ (C–F). '1st' is the first current trace elicited after verapamil wash-in and 'acc' indicates the current after accumulation of block. The interpulse-interval was 30 s. The peak currents shown in A, C and E were normalized and plotted against the time during the experiment in B, D and F, respectively.

when using high $[Na^+]_o$ (Figure 2C). Inactivation of the control current in high $[K^+]_o$ without verapamil was slower ($\tau_{inact} = 620 \pm 250$ ms; $n = 12$) compared to when measured in high $[Na^+]_o$. If verapamil was added, the peak current of the first pulse was smaller, similar to the measurements in high $[Na^+]_o$, and current decay was accelerated, too. Accumulation of block, seen in the reduction of peak currents during repetitive depolarizations, however, was less pronounced than in high $[Na^+]_o$ (see Figure 2D).

To see if there is a link between inactivation, recovery from inactivation and accumulation of verapamil block we tested verapamil on the H404T mutant Kv1.3 channel. The inactivation of this mutant was very slow compared to wild type (τ_{inact} several seconds in high $[K^+]_o$), not complete and connected to a fast recovery from inactivation. The time constant for recovery from block was less than 1 s for this mutant channel compared to 78 s or 15 s for the wild type in high $[Na^+]_o$ or high $[K^+]_o$, respectively. The current decay of the H404T mutant channel during depolarization in the presence of verapamil, shown in Figure 2E, was qualitatively similar to wild type; however, steady-state currents at the end of the depolarization were clearly detectable. The steady-state currents were smaller the higher the verapamil concentration. In addition, in the H404T mutant no further reduction of peak currents beyond the first pulse after verapamil wash-in was observed (see Figure 2F). We assume that the peak

current reduction of the first current trace after verapamil application was caused by open channel block, i.e. development of open channel block before not all channels have opened (analogous to wild type). After that, no accumulation of block occurred in the H404T mutant channel, even if we increased the pulse rate from 2 min^{-1}, as used for the accumulation of block in wild type and in Figure 2B,D,F, to 30 min^{-1} (data not shown).

The results presented in Figure 2 suggest that accumulation of block might only be possible if channels show accumulation of inactivation.

The absorbing state

To quantify the transition from the open-blocked state (OB; see Figure 1, scheme I) into the absorbing state (IB), a transition that is electrically silent, we measured tail currents in response to different durations of the depolarizing pulse. Figure 3A,C and E show superimposed tail currents elicited by depolarizing test pulses with varying durations for the wild type under control (high $[K^+]_o$) conditions (Figure 3A) and with verapamil (Figure 3C), and for the mutant H404T under similar (high $[K^+]_o$) conditions with verapamil (Figure 3E). For the wild type, test pulses longer than 40 ms decreased the peak current amplitude of the tail current the longer the duration of the test pulse (Figure 3A,C). The resulting tail current integrals are plotted against the pulse duration in Figure 3B,D and F, respectively. We used the integral to determine those channels that were in states OB and O, while IB-channels might recover too slowly to carry significant current during these measurements. The decrease of the peak current amplitude of the tail currents and the

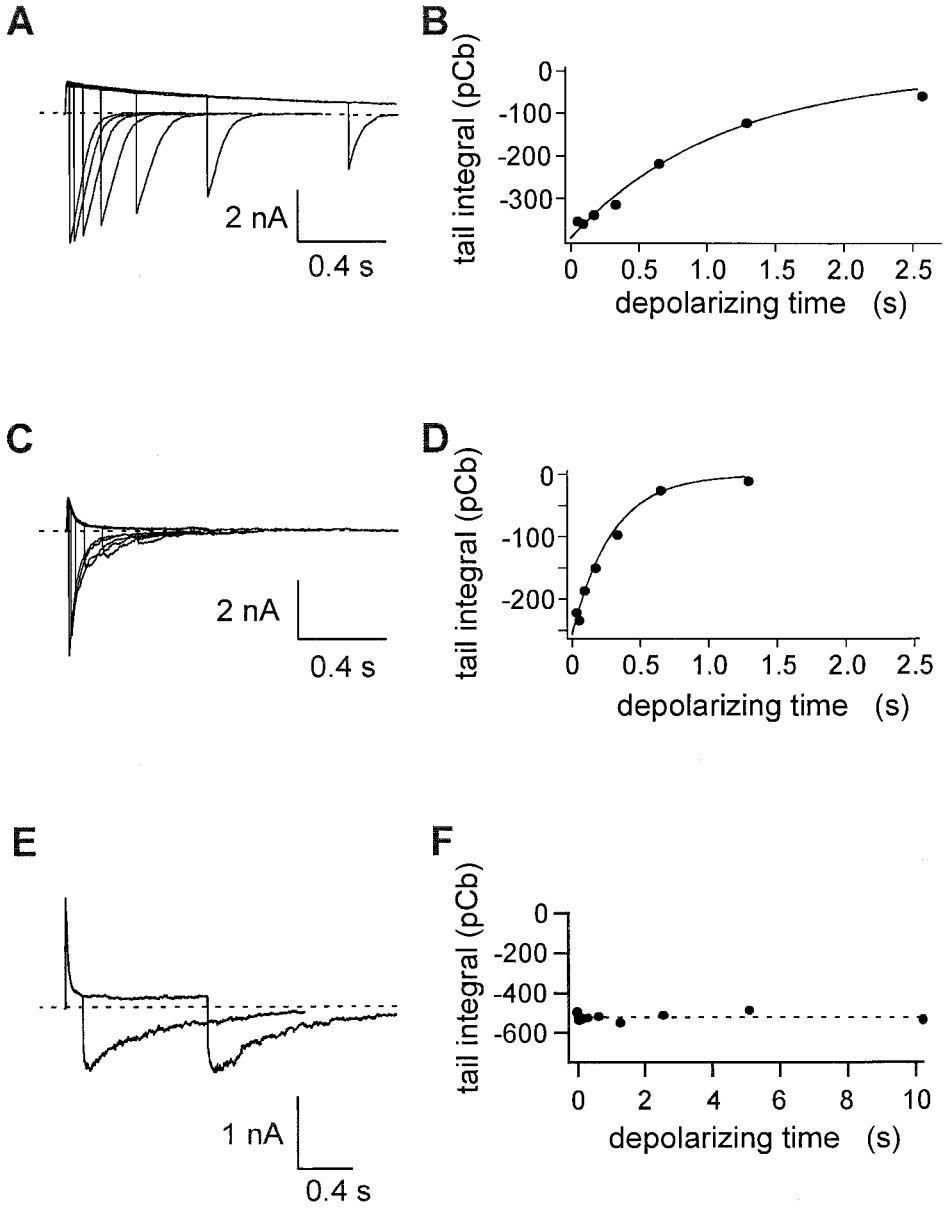

Figure 3 Inactivation of blocked channels. Tail currents in high $[K^+]_o$ were elicited by a pulse to −80 mV after variable durations of depolarization to 40 mV in the absence (A) and presence of 50 μM verapamil (C). In B and D the corresponding integrals of the tail currents (measured in picoCoulomb) were plotted against the duration of the depolarizing pulse and a mono-exponential function was fitted to the data for depolarizations longer than 40 ms. E, tail currents elicited in the H404T mutant in high $[K^+]_o$ and 50 μM verapamil were independent of the applied duration of depolarization, here 200 and 1250 ms, respectively. In F the corresponding integrals of those and similar tail currents shown in E were plotted against the duration of the depolarizing pulse. The dotted line is drawn for clarity at a constant integral of −520 pCb.

decrease of the tail current integrals with depolarizations longer than 40 ms, in the presence and absence of verapamil, could be fitted with mono-exponential functions. Under control conditions (Figure 3A) the time constant of this decrease in the tail current integral was 760 ± 91 ms ($n=8$). This value was not significantly different from the mono-exponential inactivation time course obtained by a fit to the current decay during depolarization in high $[K^+]_o$ $\tau_{inact} = 620 \pm 250$ ms ($n=12$). In the presence of 50 μM verapamil the time constant of the decrease of the tail current integrals was significantly ($P=0.005$) smaller (230 ± 91 ms; $n=8$; Figure 3D) than under control conditions consistent with the hypothesis that verapamil binding accelerates channel inactivation. An alternative interpretation, however, involving a more indirect effect of verapamil on channel inactivation will be presented in the discussion. In addition to the faster time constant of the decrease of the tail current integrals in verapamil compared to control measurements without verapamil it is apparent that there is a difference between the maximum–integral of the tail currents with and without verapamil (compare Figure 3B and D). This difference of about 100 pC, however, may result from the transition of blocked channels into the absorbing (inactivated) state starting at a time when not all the channels have been blocked yet.

In contrast to wild type, the tail currents of the mutant H404T channels were independent of the duration of the depolarizing pulse (Figure 3E and F). Therefore, no transition from the open-blocked state (OB) into an absorbing (inactivated) state (IB) seemed to happen in the mutant channel according to the simplified scheme II (Figure 1), where neither an intrinsic inactivated (I) nor a blocked-inactivated (IB) state exists.

In conclusion, the inactivated-blocked state (IB) seems to be responsible for the accumulation of the verapamil block in the wild type *m*Kv1.3 and this state can be reached from the open-blocked state (OB). The following experiment should demonstrate that the transition O→I→IB is also possible. Since both states, either I or IB are electrically silent, only an indirect test could be performed to estimate this transition (Figure 4). The experiment had three settings, at all times the cells were depolarized for 2.5 s at 40 mV to inactivate all channels. The cells were then repolarized to −80 mV for 20 s and finally depolarized again for 50 ms to 40 mV again to elicit the test current. If high $[Na^+]_o$ without verapamil was the bathing solution, over 75% of the channels recovered from the 2.5 s depolarizing pulse to 40 ms after the 20 s as can be seen in Figure 4B by the ratio of peak current amplitudes elicited with the 50 ms pulse in comparison to the peak current amplitude elicited with the 2.5 s depolarization to 40 mV (Figure 4E, upper bars). If high $[Na^+]_o$ with 50 μM verapamil was the bathing solution during both depolarizations (Figure 4D), only $23 \pm 4.4\%$ ($n=7$) did recover (Figure 4E, lower bars). To test the affinity of verapamil only for the inactivated channels, verapamil was applied after the first 2 s of the 2.5 s depolarizing pulse, i.e. at a time where most of the channels should be in the inactivated state. This manoeuver, shown in Figure 4C, resulted in a fraction of channels that were available for opening after 20 s (Figure 4E, middle bar) of $32 \pm 7.8\%$ ($n=3$). This fraction was not significantly different ($P=0.5$) from the fraction obtained if verapamil was present throughout the 2.5 s depolarizing pulse. Therefore we conclude that it is not necessary for verapamil binding to go through the open (O) and then open-blocked (OB) state to reach the inactivated-blocked (IB) state. This also suggests that the inactivated channel provides access to the binding site and has an affinity for verapamil similar to the open channel conformation.

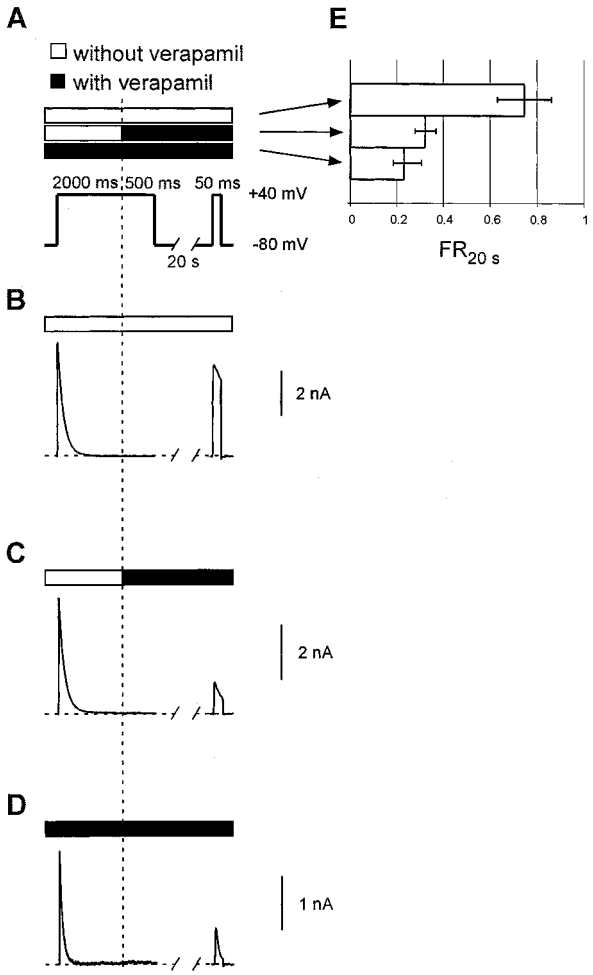

Figure 4 Affinity of verapamil to inactivated channels. (A) To test access and affinity of the inactivated channels to verapamil, the indicated pulse protocol was applied while the channels were bathed in high $[Na^+]_o$ either with or without verapamil. In one experimental setting, after 2 s of depolarization, when most of the channels were inactivated, the local verapamil concentration was increased using a picospritzer-system (pipette solution: high $[Na^+]_o$ containing 50 μM verapamil). (B–D) Original current traces elicited with the pulse and solution change setting shown and described in A. (E) The recovery of inactivated or inactivated-block channels after 20 s ($FR_{20\,s}$) was measured as the ratio of the peak current amplitudes elicited during the two depolarizations 20 s apart.

Voltage dependence of block

Although onset of verapamil block is described to be voltage independent (Catacuzzeno *et al.*, 1999) or only weakly dependent on the depolarizing voltage (DeCoursey, 1995: 138 mV per e-fold), we found a steep voltage dependence of unblock. Off-rate constants for different repolarization potentials were determined from those and similar tail currents of wild type channels as shown in Figure 5A and plotted as a function of the repolarization potential (Figure 5B). It is obvious from Figure 5B that the off-rate constant for verapamil to leave its binding site is strongly voltage dependent at voltages more negative than −60 mV. The dotted line in Figure 5B represents a mono-exponential fit to the data with −36 mV per e-fold for the wild type *m*Kv1.3 channel (in the H404T mutant channels a voltage dependence

of −37 mV per e-fold resulted). An extrapolation to 40 mV, the used depolarization potential, gives $l \sim 0.3\ s^{-1}$ for wild type and is not in agreement with the data expected from the simulations (see Table 1, Figure 5B: point at 40 mV). A better fit resulted from the assumption of an additional, voltage-independent fraction, according to: $l(V) = N + P*\exp(-V/27\ mV)$, where V is the repolarization potential in (mV), N represents the product of the off-rate constant l of the unprotonated verapamil and the fraction of unprotonated verapamil; P represents the product of the off-rate constant l at V = 0 mV and the fraction of protonated verapamil.

Current simulation

To recreate the current decay during development of block and to obtain the time courses of the other states, we performed a simulation based on the scheme I and II (Figure 1) for wild type and the H404T mutant channels, respectively. Figure 6 shows the result of such a simulation. It shows in A the probabilities of the states of wild type channels, determined using scheme I (Figure 1). One can see that during the development of verapamil block at 40 mV in high $[Na^+]_o$ most channels go into the open-blocked state (OB) after opening. After that the transition into the slowly recovering inactivated and blocked state happens (OB→IB), where over 90% of the channels will be at the end of the 400 ms pulse. Therefore, recovery from block in high $[Na^+]_o$ is slow and mono-exponential (data not shown, $\tau \sim 78$ s).

In high $[K^+]_o$ (Figure 6B), transition of OB-channels into IB is slower compared to the transition in high $[Na^+]_o$ and less complete. Recovery from block is therefore bi-exponential with a fast recovery time course representing recovery of OB channels ($\tau \sim 100$ ms), and a slow time course representing recovery of IB-channels ($\tau \sim 15$ s; data not shown). The

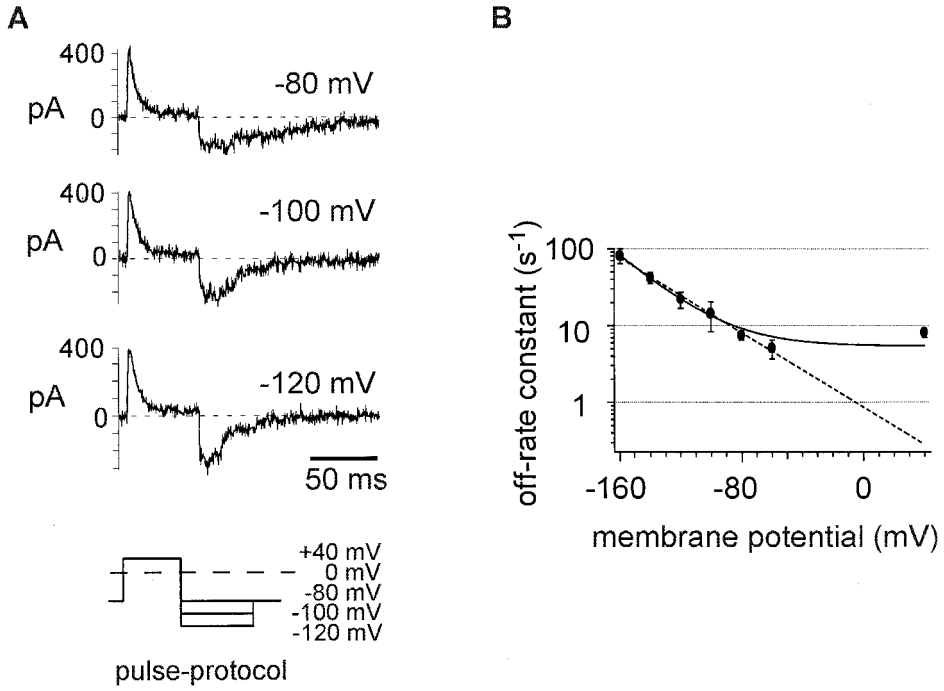

Figure 5 Voltage dependence of unblock. (A) At hyperpolarizing voltages the hooks got more pointed as the result of the voltage dependence of deactivation and off-rate constant l. To quantify l at different repolarization-potentials, we used the pulse protocol, given in the figure (100 ms depolarization at 40 mV), and fitted mono-exponential functions to the rising part of the tail currents. In C, l is plotted against the repolarizing potential on a semilogarithmic scale (means ± s.d., $n = 5$). The mono-exponential fit (dotted line, only taking into account the negative potentials) is extrapolated to the depolarizing potential 40 mV, resulting in $l \sim 0.3\ s^{-1}$. A better match, especially for the off-rate constants calculated for V = 40 mV, comes from the assumption of a fit, that consists of the sum of a mono-exponential function and a constant value: $l(V) = N + P*\exp(-V/27\ mV)$, with $N = 5.4\ s^{-1}$ and $P = 0.19\ s^{-1}$, where V is the repolarization potential in (mV). N represents the product of the off-rate constant l of the unprotonated verapamil and the fraction of unprotonated verapamil. P represents the product of the off-rate constant l at V = 0 mV and the fraction of protonated verapamil.

Table 1 Summary of verapamil block constants deduced from the currents and the simulations as given in Methods

	wild type m*Kv1.3*		*H404T mutant* m*Kv1.3*	
	high $[Na^+]_o$	*high* $[K^+]_o$	*high* $[Na^+]_o$	*high* $[K^+]_o$
$k(mol^{-1}s^{-1})$	2.5 ± 0.93 * 10^6 ($n = 13$)	1.7 ± 0.65 * 10^6 ($n = 8$)	1.8 ± 0.47 * 10^6 ($n = 15$)	1.5 ± 0.27 * 10^6 ($n = 10$)
$l_{(-80\ mV)}$ (s^{-1})	n.d.	7.5 ± 1.1 ($n = 5$)	n.d.	7.2 ± 2.1 ($n = 3$)
$l_{(40\ mV)}$ (s^{-1})	7.1 ± 2.0 ($n = 10$)	8.2 ± 1.4 ($n = 9$)	4.2 ± 2.0 ($n = 15$)	6.5 ± 1.6 ($n = 10$)
K_d (μM)	2.8	4.8	2.3	4.3
τ_{inact} (ms)	220 ± 91 ($n = 42$)	620 ± 250 ($n = 12$)	> 1000	> 1000
$\tau_{inact\ vera}$ (ms)	~30 ± 14 (n = 10)	230 ± 91 ($n = 8$)	n.d.	> 1000
$\tau_{rec\ inact\ (-80\ mV)}$ (s)	15 ± 4.9 ($n = 18$)	10 ± 3.1 ($n = 6$)	< 1	< 1
$\tau_{rec\ block\ (-80\ mV)}$ (s)	78 ± 16 ($n = 7$)	15 ± 3.3 ($n = 5$)	1.1 ± 0.47 ($n = 3$)	0.34 ± 0.085 ($n = 5$)

Values are given as mean ± s.d. (n = number of experiments); abbreviations and derivations are explained in Methods. K_d was calculated from the mean values of $l_{(40\ mV)}$ and $k_{(40\ mV)}$.

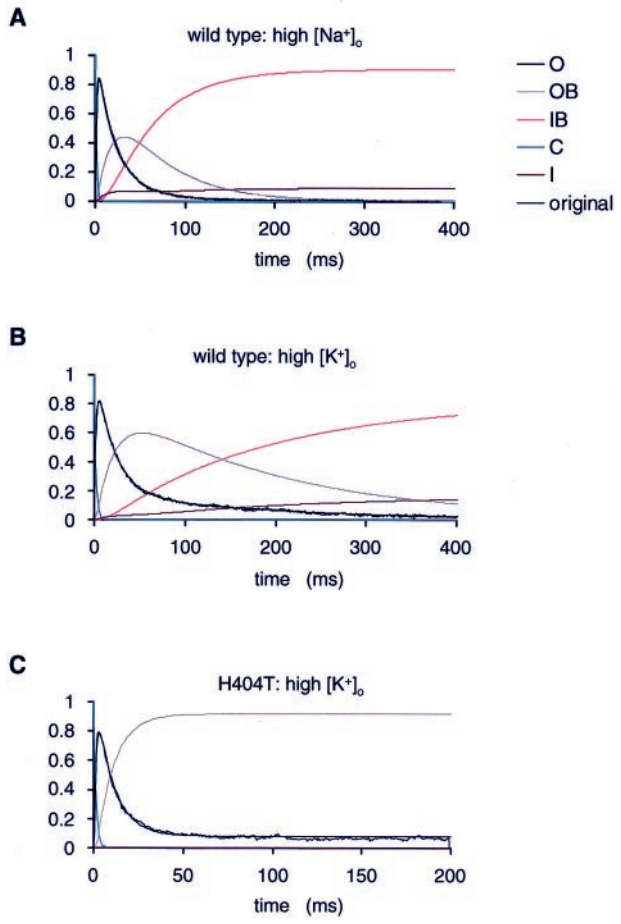

Figure 6 Simulation of block-onset. Simulated currents in the presence of verapamil (wild type: (A) 20 μM verapamil in high $[Na^+]_o$; (B) 50 μM verapamil in high $[K^+]_o$ according to scheme I of Figure 1. H404T mutant: (C) 50 μM verapamil in high $[K^+]_o$ according to scheme II of Figure 1), as expected for a depolarizing pulse to 40 mV from a holding potential, that has allowed complete recovery from block. A representative original scaled current through *m*Kv1.3 is superimposed in the same bathing conditions. The used constants were: (A) $\alpha = 0.5\ ms^{-1}$; $h = 7.0\ s^{-1}$; $j = 0.1\ s^{-1}$; $k' = 40\ s^{-1}$; $l = 4.0\ s^{-1}$; $h^* = 20\ s^{-1}$; $j^* = 0.1\ s^{-1}$. (B) $\alpha = 0.4\ ms^{-1}$; $h = 1.3\ s^{-1}$; $j = 0.1\ s^{-1}$; $k' = 44\ s^{-1}$; $l = 7.0\ s^{-1}$; $h^* = 5.0\ s^{-1}$; $j^* = 0.38\ s^{-1}$. (C) $\alpha = 0.55\ ms^{-1}$; $k'_{(40\ mV)} 90\ s^{-1}$; $l_{(40\ mV)} = 7.5\ s^{-1}$.

relative fraction of the occupancy of OB compared to IB depends strongly on the duration of the depolarization.

Figure 6c shows the simulation of the H404T mutant Kv1.3 channels according to scheme II (Figure 1). A direct equilibration between the open and the open-blocked state, resulting in a steady-state current can clearly be seen. According to scheme II (Figure 1) no transition into any absorbing (inactivated) state exists, and, as a consequence, recovery from block is mono-exponential and fast ($\tau \sim 340$ ms in high $[K^+]$).

A summary of all the block constants deduced from the currents and the simulations as given in Methods is shown in Table 1.

Discussion

Our main goal was to provide evidence that the absorbing state observed through the accumulation of verapamil block was identical to the inactivated and blocked state, as suggested first by DeCoursey (1995). In this paper we present additional evidence to support this hypothesis.

The H404T mutant mKv1.3 channel

To do so, we used the H404T mutant *m*Kv1.3 channel known for its slow inactivation (Aiyar *et al*., 1995; Rauer & Grissmer, 1996). The mutated amino acid H404 is located near the outer vestibule in the S5S6-linker and was originally described to be the receptor site for externally applied TEA^+ (MacKinnon & Yellen, 1990; Kavanaugh *et al*., 1991; 1992). The amino acid at this position is therefore directed away from the common binding site (S6, P-loop) for blockers that act from the cytoplasmic side of the channel, like internally applied TEA^+, quinidine and 4-amino pyridine. Verapamil too is supposed to bind at or near this intracellularly located site (Rauer & Grissmer, 1996; 1999). If, in the mutant channel, only inactivation is disrupted with unchanged open block properties, we would expect three differences in block by verapamil compared to wild type channels: (i) steady-state currents should be detected; (ii) the integrals of the tail currents should not depend on the duration of the depolarizing pulse; and (iii) verapamil block should not accumulate. All three differences were indeed observed. The different blocking behaviors of wild type and H404T mutant *m*Kv1.3 channel by the phenylalkylamine verapamil could be attributed to comparable open block properties, as the on- and off-rate constants were similar in both channels. The apparent differences in block (steady-state, tail-integrals, recovery, accumulation) of both channels were caused by the absence of intrinsic C-type inactivation in the H404T mutant channel (compare scheme I and II, Figure 1). Therefore we concluded that the absorbing state of verapamil block must be identical to the intrinsic inactivated and blocked state (IB).

Verapamil indirectly promotes inactivation

From our experiments of the decrease of the tail current integrals in the presence of verapamil and from modeling open-block currents we obtained time constants for inactivation that were smaller in the presence of verapamil ($\tau_{inact\ vera}$) than the time constants of the fits of the C-type inactivating channels without verapamil (τ_{inact}; in high $[K^+]_o$ by a factor ~ 3, in high $[Na^+]_o$ even higher, see Table 1). Several possibilities could account for this faster inactivation rate with verapamil. (i) In analogy to D600 action on L-type Ca^{2+} channels Hering *et al*. (1997) proposed that for block of the L-type Ca^{2+} channel by the PAA D600 the faster inactivation observed with D600, in combination with the fact that deactivation in the presence of D600 was impossible, was due to the drug keeping the channel in an open-blocked conformation (see Figure 1, scheme I). Therefore, in the case for D600 action on L-type Ca^{2+} channels, inactivation rate did increase with an unchanged inactivation-rate constant because the probability increased to be in a state, from which inactivation can occur. (ii) Another mechanism was presented by Baukrowitz & Yellen (1996) on Shaker potassium channels. They showed that a blocking molecule could influence the conformational changes in the channel protein, for example by speeding up inactivation, i.e. changing the inactivation-rate constant itself. (iii) However, they also separated another distinct effect that was mediated by the disruption of the outflow of K^+. Under normal conditions, an inactivation modulating binding site for K^+ at the outer vestibule of the *m*Kv1.3 channel might be occupied by outflowing K^+. K^+ binding to this site would slow inactivation, as is the situation in high $[K^+]_o$ (Cahalan *et al*., 1985; Grissmer & Cahalan, 1989). By occluding the pore,

verapamil could disrupt the K^+-outflow thereby reducing the local $[K^+]$ at the outer vestibule. Therefore the occlusion of the pore might starve out the inactivation-modulating low-affinity binding site for K^+ (Levy & Deutsch, 1995; 1996). This in turn is expected to result in an increase of the inactivation-rate constant.

For verapamil block of *m*Kv1.3 channels we favour the third, starving theory (Baukrowitz & Yellen, 1996) for two reasons: (i) differences between inactivation time constants with (*h**) and without verapamil (*h*) are higher in low than in high $[K^+]_o$. A high $[K^+]_o$ solution could partially hinder the starving of the site and (ii) differences in recovery from block compared to recovery from inactivation are higher in low than in high $[K^+]_o$, too, perhaps for the same reason. However, we cannot rule out the other two mechanisms or a combination thereof to be responsible for the described effects.

Voltage dependence of block

Several lines of evidence had been presented that verapamil acted from inside the cell (DeCoursey, 1995; Rauer & Grissmer, 1996; 1999; Trequattrini *et al*., 1998), and that verapamil reached its binding site in the unprotonated form, according to a weak (DeCoursey, 1995: 138 mV per e-fold) or completely absent (Catacuzzeno *et al*., 1999) voltage dependence of the on-rate constant *k*. However, unblock of verapamil was faster at hyperpolarizing potentials. The voltage dependence curve of *l* could be well-fitted by the assumption of two fractions of verapamil, one fraction with a voltage independent off-rate constant and one fraction with a voltage dependent off-rate constant. Alternatively, one could assume two different binding sites for verapamil rather than two forms of the molecule binding and producing different degrees of block. However, the experiments by Catacuzzeno *et al*. (1999) on $I_{K(DR)}$ channels and N-met-verapamil showed that the off-rate is strictly voltage-dependent, missing the voltage independent part. Under the assumption that the binding sites of verapamil and N-met-verapamil are identical the hypothesis of two forms of the verapamil molecule producing the effect seems more likely. Because N and P are the product of the fraction of either protonated or unprotonated verapamil and the corresponding constant *l*, it is not possible to deduce *l* or the fractions from the fit.

From that and from the fact that hooked tail currents could only be seen in high $[K^+]_o$, indicating that hooked tail currents depend on high $[K^+]_o$ at the extracellular site, we suggest a relief of block by inflowing K-ions at hyperpolarizing voltages. This mechanism was first proposed by Armstrong (1969) for the unblock of intracellularly applied TEA^+ on delayed rectifier K^+ channels of squid giant axon. He proposed an electrostatic repulsion being responsible for 'clearing' the occluding ion from the pore, whereby inflowing K^+ would get accelerated, pushing the permanently charged TEA^+ off its binding site.

Block of mKv1.3 vs block of L-type Ca^{2+} channels

Verapamil block of L-type Ca^{2+} channels has also been shown to be state-dependent. Hering *et al*. (1997) presented a model for PAA interaction that did not allow access to the binding site as long as the activation gate was closed. In addition, Johnson *et al*. (1996) simulated the open block by PAA assuming a $K_d \sim 20-30$ times higher for the closed state than for open and inactivated states. They showed that once the channel opened, the binding site could be reached by the blocker with a $K_d \sim 1.7$ nM (D888) or 370 nM (Verapamil) (Johnson *et al*., 1996), compared with $2-5$ μM in *m*Kv1.3. Once verapamil did bind to the L-type Ca^{2+} channel its mean residency time was 2.8 s, compared with ~ 0.13 s if bound to *m*Kv1.3. This indicated, together with the fact that channels cannot close with PAA bound (no CB), that in the L-type Ca^{2+} channel inactivation rate, not rate constant, was increased. In *m*Kv1.3 channels this might not account for the observed increase in inactivation, because (i) at 40 mV Kv1.3 channels stay in the open conformation most of the time (Cahalan *et al*., 1985; Marom & Levitan, 1994) and (ii) residency time is short. That is why we propose a changed rate constant itself ($h^* > h$).

Since inactivation was speeded up by PAAs in the L-type Ca^{2+} channel it seemed that the channel might be able to reach a deep inactivated state faster once a PAA was bound compared to without PAA. Therefore the time course for recovery from block even after short depolarizations is similar to the time course for recovery from inactivation observed only after long depolarizations. In addition, in L-type Ca^{2+} channels the interaction of the PAA with the inactivated channel is discussed controversely because affinities for the states were found to be dependent on the PAA species (Johnson *et al*., 1996) and even on the permeating ions (Nawrath & Wegener, 1997; Hering *et al*., 1997). However, a trapping of the PAA in the inactivated *m*Kv1.3 channel, as reported for L-type Ca^{2+} channels (Hering *et al*., 1997), might be ruled out by our experiments, because in Figure 4 the I-state was thought to provide access to the verapamil. Similarly, simulations of recovery from verapamil block resulted in a slower time course compared to recovery from inactivation, even if affinities of verapamil to states O and I were identical, as was expected for the verapamil block of *m*Kv1.3 according to scheme I (Figure 1).

Finally, Hering *et al*. (1998) showed a direct correlation between the inactivation of the Ca^{2+} channel and the extend of PAA block accumulation ($r = 0.92$). Our results on a voltage-gated potassium channel, Kv1.3, presented in this paper, support and extend these findings indicating an essential role of an intrinsic inactivated state of the channel for the accumulation of PAA block.

In conclusion, we investigated the state-dependent manner of *m*Kv1.3 block by the PAA verapamil and concluded from our results that verapamil cannot block the closed state of *m*Kv1.3 but is able to block the open as well as the inactivated state of the channel with similar potency. The accumulation of block of verapamil seems to be unequivocally connected to the inactivated state of the channel. In addition, in order to produce new PAA-derivatives, which are Kv1.3-selective over L-type Ca^{2+} channels, the H404T mutant *m*Kv1.3 channels could be used to search for open-channel blocking drugs in high through-put screens.

The authors would like to thank Ms Katharina Ruff for her excellent technical assistance. This work was supported by grants from the DFG (Gr 848/4-2; Gr 848/8-1) and the BMBF (iZKF Ulm, B7).

References

AIYAR, J., WITHKA, J.M., RIZZI, J.P., SINGLETON, D.H., ANDREWS, G.C., LIN, W., BOYD, J., HANSON, D.C., SIMON, M., DETHLEFS, B., LEE, C., HALL, J.E., GUTMAN, G.A. & CHANDY, K.G. (1995). Topology of the pore-region of a K^+ channel revealed by the NMR-derived structures of scorpion toxins. *Neuron,* **15,** 1169–1181.

ARMSTRONG, C.M. (1969). Time course of TEA^+-induced anomalous rectification in squid giant axons. *J. Gen. Physiol.,* **50,** 491–503.

BAUKROWITZ, T. & YELLEN, G. (1996). Use-dependent and exit rate of the last ion from the multi-ion pore of a K^+ channel. *Science,* **271,** 653–656.

CAHALAN, M.D. & CHANDY, K.G. (1997). Ion channels in the immune system as targets for immunosuppression. *Curr. Opin. Biotechnol.,* **8,** 749–756.

CAHALAN, M.D., CHANDY, K.G., DECOURSEY, T.E. & GUPTA, S. (1985). A voltage-gated potassium channel in human T lymphocytes. *J. Physiol.,* **358,** 197–237.

CATACUZZENO, L., TREQUATTRINI, C., PETRIS, A. & FRANCIOLINI, F. (1999). Mechanism of verapamil block of a neuronal delayed rectifier K channel: active form of the blocker and location of its binding domain. *Br. J. Pharmacol.,* **126,** 1699–1706.

CHANDY, K.G., DECOURSEY, T.E., CAHALAN, M.D., MCLAUGHLIN, C. & GUPTA, S. (1984). Voltage-gated potassium channels are required for human T lymphocyte activation. *J. Exp. Med.,* **160,** 369–385.

CHANDY, K.G., GUTMAN, G.A. & GRISSMER, S. (1993). Physiological role, molecular structure and evolutionary relationships of voltage-gated potassium channels in T lymphocytes. *The Neurosciences,* **5,** 125–134.

DECOURSEY, T.E. (1990). State-dependent activation of K^+ currents in rat type II alveolar epithelial cells. *J. Gen. Physiol.,* **95,** 617–646.

DECOURSEY, T.E. (1995). Mechanism of K^+ channel block by verapamil and related compounds in rat alveolar epithelial cells. *J. Gen Physiol.,* **106,** 745–779.

DECOURSEY, T.E., CHANDY, K.G., GUPTA, S. & CAHALAN, M.D. (1984). Voltage-gated K^+ channels in human T lymphocytes: a role in mitogenesis? *Nature,* **307,** 465–468.

DURELL, S.R. & GUY, H.R. (1996). Structural model of the outer vestibule and selectivity filter of the Shaker voltage-gated K^+ channel. *Neuropharmacology,* **35,** 761–773.

ECCLESTON, E., LEONARD, B.J., LOWE, J.S. & WELFORD, H.J. (1973). Basophilic leukaemia in the albino rat and a demonstration of the basopoietin. *Nat. New Biol.,* **244,** 73–76.

GRISSMER, S. & CAHALAN, M.D. (1989). Divalent ion trapping inside potassium channels of human T lymphocytes. *J. Gen. Physiol.,* **93,** 609–630.

GRISSMER, S., DETHLEFS, B., WASMUTH, J.J., GOLDIN, A.L., GUTMAN, G.A., CAHALAN, M.D. & CHANDY, K.G. (1990). Expression and chromosomal localization of a lymphocyte K^+ channel gene. *Proc. Natl. Acad. Sci. U.S.A.,* **87,** 9411–9415.

HAMILL, O.P., MARTY, A., NEHER, E., SAKMANN, B. & SIGWORTH, F.J. (1981). Improved patch-clamp techniques for high-resolution current recording from cells and cell-free membrane patches. *Pflügers Arch.,* **391,** 85–100.

HERING, S., ACZEL, S., KRAUS, R.L., BERJUKOW, S., STRIESSING, J. & TIMIN, E.N. (1997). Molecular mechanism of use-dependent calcium channel block by phenylalkylamines: role of inactivation. *Proc. Natl. Acad. Sci. U.S.A.,* **94,** 13323–13328.

HERING, S., BERJUKOW, S., ACZEL, S. & TIMIN, E.N.. (1998). Ca^{2+} channel block and inactivation: common molecular determinants. *Trends Pharmacol. Sci.,* **19,** 439–443.

HOCKERMAN, G.H., JOHNSON, B.D., ABBOTT, M.R., SCHEUER, T. & CATTERALL, W.A. (1997). Molecular determinants of high affinity phenylalkylamine block of L-type calcium channels in transmembrane segment IIIS6 and the pore region of the alpha1 subunit. *J. Biol. Chem.,* **272,** 18759–18765.

HOCKERMAN, G.H., JOHNSON, B.D., SCHEUER, T. & CATTERALL, W.A. (1995). Molecular determinants of high affinity phenylalkylamine block of L-type calcium channels. *J. Biol. Chem.,* **270,** 22119–22122.

JACOBS, E.R. & DECOURSEY, T.E. (1990). Mechanisms of potassium channel block in rat alveolar epithelial cells. *J. Pharmacol. Exp. Ther.,* **255,** 459–472.

JOHNSON, B.D., HOCKERMAN, G.H., SCHEUER, T. & CATTERALL, W.A. (1996). Distinct effects of mutations in transmembrane segment IVS6 on block of L-type calcium channels by structurally similar phenylalkylamines. *Mol. Pharmacol.,* **50,** 1388–1400.

KAVANAUGH, M.P., HURST, R.S., YAKEL, J., VARNUM, M.D., ADELMAN, J.P. & NORTH, R.A. (1991). Interaction between tetraethylammonium and amino acid residues in the pore of cloned voltage-dependent potassium channels. *J. Biol. Chem.,* **266,** 7583–7587.

KAVANAUGH, M.P., VARNUM, M.D., OSBORN, P.B., CHRISTIE, M.J., BUSCH, A.E., ADELMAN, J.P. & NORTH, R.A. (1992). Multiple subunits of a voltage-dependent potassium channel contribute to the binding site for tetraethylammonium. *Neuron,* **8,** 493–497.

KOO, G.C., BLAKE, J.T., TALENTO, A., NGUYEN, M., LIN, S., SIROTINA, A., SHAH, K., MULVANY, K., HORA, D.J., CUNNINGHAM, P., WUNDERLER, D.L., MCMANUS, O.B., SLAUGHTER, R., BUGIANESI, R., FELIX, J., GARCIA, M., WILLIAMSON, J., KACZOROWSKI, G., SIGAL, N.H., SPRINGER, M.S. & FEENEY, W. (1997). Blockade of the voltage-gated potassium channel Kv1.3 inhibits immune responses in vivo. *J. Immunol.,* **158,** 5120–5128.

KRIEG, P.A. & MELTON, D.A. (1984). Functional messenger RNAs are produced by SP6 in vitro transcription of cloned cDNAs. *Nucleic Acids Res.,* **12,** 7057–7070.

LEVY, D.I. & DEUTSCH, C. (1995). Recovery from C-type inactivation is modulated by extracellular potassium. *Biophys. J.,* **70,** 798–805.

LEVY, D.I. & DEUTSCH, C. (1996). A voltage dependent role for K^+ in recovery from C-type inactivation. *Biophys. J.,* **71,** 3157–3166.

MACKINNON, R. & YELLEN, G. (1990). Mutations affecting TEA blockade and ion permeation in voltage-activated K^+ channels. *Science,* **250,** 276–279.

MAROM, S. & LEVITAN, I.B. (1994). State-dependent inactivation of the Kv3 potassium channel. *Biophys. J.,* **67,** 579–589.

NAWRATH, H. & WEGENER, J.W. (1997). Kinetics and state-dependent effects of verapamil on cardiac L-type calcium channels. *Naunyn Schmiedebergs Arch. Pharmacol.,* **355,** 79–86.

RAUER, H. & GRISSMER, S. (1996). Evidence for an internal phenylalkylamine action on the voltage-gated potassium channel Kv1.3. *Mol. Pharmacol.,* **50,** 1625–1634.

RAUER, H. & GRISSMER, S. (1999). The effect of deep pore mutations on the action of phenylalkylamines on the Kv1.3 potassium channel. *Br. J. Pharmacol.,* **127,** 1065–1074.

RÖBE, R. & GRISSMER, S. (1999). The role of the intrinsic inactivation in the accumulation of phenylalkylamine block in *m*Kv1.3. *Pflügers Arch.,* **437,** R72.

RÖBE, R. & GRISSMER, S. (2000). Detailed characterization of verapamil block of *m*Kv1.3. *Pflügers Arch.,* **439,** R405.

STRIESSNIG, J., GLOSSMANN, H. & CATTERALL, W.A. (1990). Identification of a phenylalkylamine binding region within the alpha 1 subunit of skeletal muscle Ca^{2+} channels. *Proc. Natl. Acad. Sci. U.S.A.,* **87,** 9108–9112.

TREQUATTRINI, C., CATACUZZENO, L., PETRIS, A. & FRANCIOLINI, F. (1998). Verapamil block of the delayed rectifier K current in chick embryo dorsal root ganglion neurons. *Pflügers Arch.,* **453,** 503–510.

(Received July 17, 2000
Revised September 18, 2000
Accepted September 19, 2000)